FATIGUE DETERIORATION PROCESS OF BRICK MASONRY AND LIFE-CYCLE ASSESSMENT OF MASONRY ARCH BRIDGES

A.K. Tomor[1] and S. De Santis[2]
[1] Senior Lecturer, Department of Construction and Property, University of the West of England, Bristol, BS16 1QY, UK, adrienn.tomor@uwe.ac.uk
[2] Research Assistant, Roma Tre University, Department of Engineering, 00146 Rome, Italy, stefano.desantis@uniroma3.it

ABSTRACT
The long-term fatigue deterioration process of brick masonry has been studied under quasi-static and high-cycle fatigue loading through a series of small-scale laboratory tests. Stages and characteristics of fracture development under compression and shear were investigated with the help of acoustic emission technique during both static and cyclic loading. Fatigue test results for compression and shear were presented in the form of S-N curves and mathematical models proposed to identify the relationships between stress level and fatigue life. The concept of fatigue limit state and permissibility limit state were discussed and related to masonry arch bridges.

KEYWORDS: fatigue, masonry, acoustic emission, fracture propagation, deterioration, masonry arch bridges

INTRODUCTION
The paper investigates characteristics of the fatigue deterioration processes of historical brick masonry under quasi-static and high-cycle fatigue loading. A dedicated small-scale laboratory test series have been undertaken at the University of the West of England, Bristol, UK to provide a set of preliminary test data for compression and shear in order to develop S-N curves for brick masonry. While there is a wealth of literature available on the fatigue behavior of concrete, metals and polymers, very little information exists on the fatigue behaviour of masonry. Material testing under fatigue loading has been carried out by Roberts [1], Abrams [2], Brencich [3], Ronca [4], AlShebani [5] and Tomor [6] under laboratory conditions and reviewed by Wang [7]. Large-scale fatigue tests have been carried out by Melbourne [8] on masonry arches and basic principles for assessing the fatigue capacity of masonry have been proposed by Clark [9], Choo [10] and Melbourne [11,12] on the structural level.

While application of the fatigue behaviour of masonry may be relevant for a range of applications, findings will be considered in relationship with masonry arch bridges in the traffic network. Masonry arch bridges represent 40% of bridges in the European traffic network, 60% of which are over 100 years old. Despite the significant increase in weight, speed and density of traffic in recent decades, masonry bridges continue to be used without any change to their original form. Naturally, long-term traffic loading will eventually lead to gradual deterioration of the bridge's fabric. Better understanding of the fatigue behaviour of masonry can help identify the residual strength and remaining service life for masonry bridges and improve life-cycle assessment. The safe fatigue limit for masonry is currently suggested to be around 50% of the

ultimate limit by UK guidelines for masonry arch bridge assessment [13], but long-term fatigue tests on masonry arches indicated significantly lower values [11]. Instead of the ultimate, a permissible limit has been suggested for bridges [12] to help ensure that working stress levels do not unexpectedly reduce the life-expectancy. There are a range of techniques available [14,15,16,17,18,19] to assess the capacity of masonry arch bridges, but all assessment techniques are based on static test data. For life cycle assessment of masonry arch bridges a Sustainable Masonry Arch Resistance Technique (SMART) has been proposed [12], through which the long-term service life and permissible loading limits may be identified. The method is in its infancy and requires large volumes of fatigue test data before it can be applied in the field.

Acoustic emission (AE) monitoring is widely used for concrete, steel and composite structures and bridges to identify internal condition, damage propagation and the structure's response to live loading, prior to effects of any damage being visible or measurable on the surface. The use of AE for masonry is however very limited due to its heterogeneous nature. A small range of studies has been carried out on AE by Verstrynge [20,21], Melbourne [22], Tomor [23], Carpinteri [24,25] under laboratory conditions and by Shigeishi [26], De Santis [27] and Masera [28] under field conditions for bridges. More research is however needed to adapt the technique for masonry and provide qualitative and quantitative guidelines.

TEST SETUP

Material properties of historical masonry varies widely. While it is impossible to consider all types of brickwork within the test series, a selection of solid weak, medium and strong bricks were chosen to represent a range of different masonry types, such as a) weak: Michelmarsh, Handmade ATR, manufacturer's published indicative strength > 6 N/mm^2, b) medium: Wienerberger Warnham Terracotta, indicative strength > 12 N/mm^2 and c) strong: Wierneberger Staffordshire Smooth Red, indicative strength > 60 N/mm^2. The three brick types were tested under compression with the help of acoustic emission (AE) monitoring to gain some indication of the range of crack propagation characteristics. Bricks were tested between layers of 3 mm plywood and load was applied using a 250 kN hydraulic loading system. As strong bricks exceeded the capacity of the loading machine, they were tested as half bricks.

Medium strength Wienerberger Warnham Red solid bricks (213×100×65 mm^3) were subsequently used to build a series of prisms and triplets (Figure 1), with average compressive strength (S_{Av}) = 22.6 N/mm^2 (standards deviation (SD) = 2.3 N/mm^2) and average Young's Modulus (E_{Av}) = 2895 N/mm^2 (SD = 260 N/mm^2). 1:1:6 cement-hydrated lime (NHL 3.5) mortar was used with 3 mm sharp washed sand by volume, with S_{Av} = 9.8 N/mm^2 (SD = 1.2 N/mm^2) and E_{Av} = 1876 N/mm^2 (SD = 258 N/mm^2). The joint thickness was 8 mm and specimens were cured for a minimum of 6 month before testing. Testing was carried out using a 250 kN hydraulic loading system supplied by Servocon Systems Ltd. Prisms were loaded under compression in the direction normal to the bed joints between layers of 3 mm plywood. Triplets were loaded under shear parallel to the bed joints with narrow steel studs positioned on either sides of the mortar joints to produce maximum shear and minimum bending.

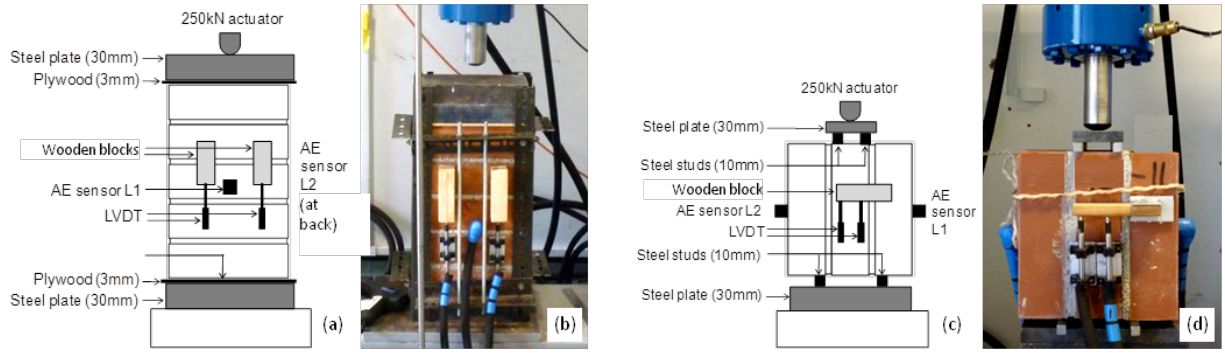

Figure 1: Prisms (a, b) and triplets (c, d)

Acoustic emission (AE) monitoring was used during the tests to monitor crack development and attempt to characterise stages of the deterioration processes. The AE technique detects high-frequency transient elastic waves that are emitted by the material during crack growth [29]. Waves are recorded on the surface by piezoelectric sensors, pre-amplified, filtered and amplified before they are processed by the data logger. AE amplitude is detected in μV, converted to AE decibel by 1 dB = 20×log (Voltage (μV) / 1 μV) [30] and energy is calculated as the area under the envelope of an AE hit. For each AE hit a number of parameters (e.g., amplitude, energy, duration, count, arrival time) and the waveform are recorded. In the current test series AE monitoring was carried out by a Physical Acoustics Micro-SAMOS system. Two 150 kHz resonant R15α sensors with 50-200 kHz operation frequency were attached to the specimens with a thin layer of hot-melt glue that has proven to be a good couplant for laboratory conditions (Figure 1). IL40s voltage preamplifiers were used with 1-400 kHz frequency bandwidth and 40 dB_{AE} gain. The AE system was calibrated using the standard method of pencil lead breaks [31]to verify the sensitivity of the sensors. The amplitude threshold was set to 35 dB_{AE} at the beginning of the tests and was progressively raised to avoid saturation. The amount of detected AE hits is naturally influenced by the applied hardware and software as well as by a range of setup-specific boundary conditions. AE results will therefore be considered qualitatively and are intended to serve as a feasibility study rather than quantitative guidelines.

STATIC LOADING OF BRICKS

In order to identify the range of signal characteristics of bricks, weak, mediums and strong bricks were tested under quasi-static compression in conjunction with AE monitoring. For the different bricks the AE patterns appear different (Figure 2), but show some similar characteristics:

- Weak brick (Figure 2a, b): relatively low and stable AE amplitude (< 70 dB_{AE}) throughout the test, with slight increase just before failure (< 80 dB_{AE}). AE energy is similarly low and stable (< 10^5 aJ) with slight increase just before failure (up to $1.5x10^5$ aJ). Sight change in the energy pattern may be observed around 20% and 92% of the maximum stress (S_{Max}).
- Medium strength brick (Figure 2c, d): large increase in amplitude and energy up to 30% S_{Max} (Phase I: < 70 dB_{AE} amplitude, < 10^5 aJ energy) and almost constant emission until failure (Phase II: < 90 dB_{AE}, < 10^6 aJ). No sudden increase in emission is visible prior to failure.
- Strong brick (Figure 2e, f): significantly higher amplitude and energy compared to weak and medium strength bricks, gradual increase up to ca. 32% S_{Max} (Phase I: < 90 dB_{AE}, < 10^6 aJ) and constant very high level emission up to failure (Phase II: < 100 dB_{AE}, < 10^7 aJ).

While studying the crack propagation characteristics of various types of bricks is outside the scope of the present paper, some similarities can be identified. Emission levels seem to increase for increasing brick strength, change in emission pattern occurs for all three brick types around 30% S_{Max}, followed by relatively stable emission and little or no further emission increase prior failure. During testing crack opening was generally observed very early on during the loading process (around or before 30% load) that suggests micro- and macro-crack development during Phase I (0-30% S_{Max}) and crack propagation, widening and crack multiplication during Phase II. Failure of the bricks was generally a gradual process and collapse occurred when insufficient material remained in place to maintain the load.

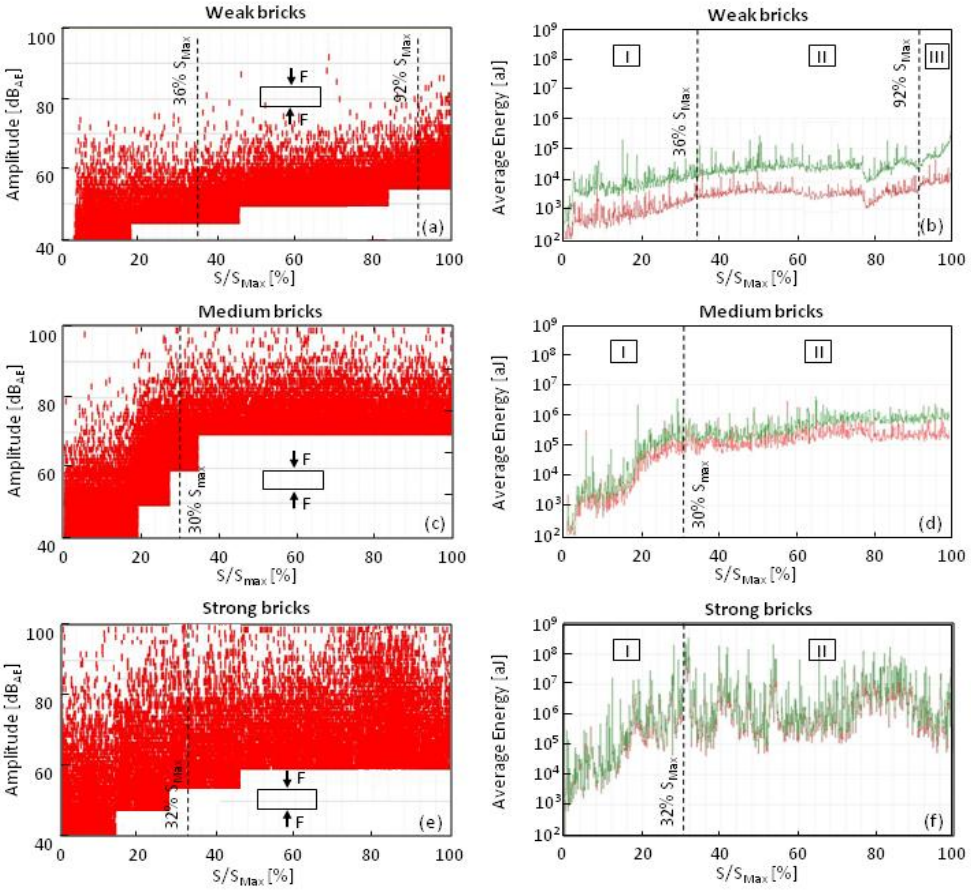

Figure 2: Bricks: weak (a,b), medium (c,d), strong (e, f); Amplitude vs. Stress (a, c, e); Average Energy (log) vs. Stress (b, d, f)

1:1:6 mortar was used in conjunction with medium strength bricks to construct prisms and triplets. A set of 100×100×100 mm^3 mortar cubes were tested under quasi-static loading together with AE monitoring (Figure 3) to allow comparison of the AE characteristics with medium strength bricks. For mortar amplitude and energy levels were typically low and stable (Phase I: < $60dB_{AE}$, < 1.5 x 10^3 aJ) throughout load application and failure was preceded by sudden increase in amplitude around 95% S_{Max} (Phase II: < $80dB_{AE}$, < 1.5 x 10^3 aJ). Amplitude and energy levels were significantly lower compared to medium strength bricks and phases of crack development up to 95% S_{Max} were difficult to distinguish.

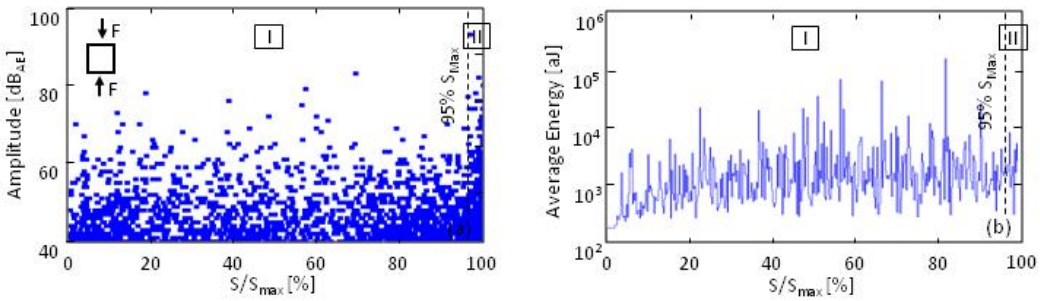

Figure 3: Mortar cube: Amplitude vs. Stress (a); Average Energy (log) vs. Stress (b)

STATIC LOADING OF PRISMS

A set of ten prisms were tested under quasi-static compressive loading with the average compressive strength of 10.8 N/mm^2 (SD = 1.0 N/mm^2). Variability of the test results was ca. 10% that is not uncommon for masonry [32]. AE amplitude and energy recordings for a typical prism are shown in Figure 4. Change in the emission pattern can be observed around 40% and 95% S_{Max}, indicating three phases of the crack development process, such as:

- Phase I: 0 - 40% S_{Max}, relatively constant low-level emission (< 60 dB_{AE}, , 10^3 aJ), similar to the crack propagation pattern of mortar shown in Figure 3. Likely to be associated with elastic deformation and compaction of the mortar.
- Phase II: 40 - 95% S_{Max}, constantly increasing emission (< 60-80 dB_{AE}, 10^3-1.5x10^5 aJ), closely resembling the emission pattern of the medium strength brick (Figure 2c, d), with two sub-sections:
  - Phase IIa: rapid amplitude and energy increase, likely to be associated with Phase I of the medium strength brick with micro- and marco-crack development (Figure 2c, d) (Phase I: < 70 dB_{AE}, < 10^5 aJ) and include macro-cracking and failure of the mortar (Figure 3) (Phase II: < 80dB_{AE}, < 1.5 x 10^3 aJ).
  - Phase IIb: reduced amplitude and energy increase, likely to be associated with Phase II of the medium strength brick and indicate crack propagation, widening and multiplication (Figure 2c, d) (Phase II: < 90 dB_{AE}, < 10^6 aJ).

  Cracking of the mortar is likely to induce local stress concentration in adjacent bricks with increasing plastic behaviour and crack propagation.
- Phase III: 95 - 100% S_{Max}, rapid emission increase (not observed in previous tests), likely to be associated with collapse of the entire specimen.

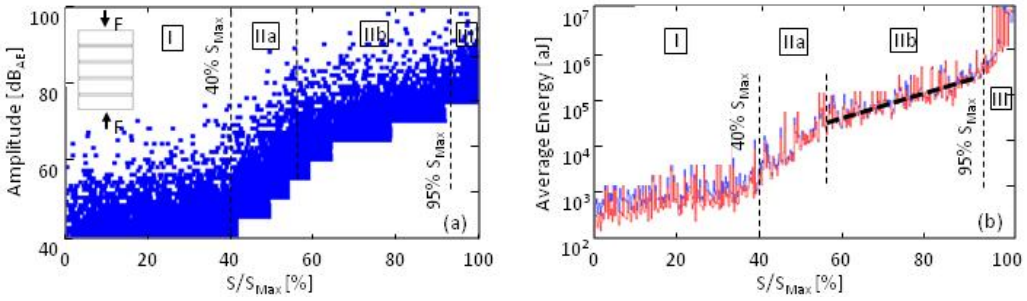

Figure 4: Prism under compression: Amplitude vs. Stress (a); Average Energy (log) vs. Stress (b)

STATIC LOADING OF TRIPLETS

A set of nine triplets were tested under quasi-static shear loading with an S_{Av} = 0.91 N/mm^2 (SD = 0.1 kN) (Figure 1c, d). Unlike bricks, mortar and prisms under compression, shear failure in triplets occurred suddenly, without any previous visual sign of damage. AE amplitude and energy recordings for a typical prism are shown in Figure 5. AE signal amplitude and energy grew gradually up to ca. 70% S_{Max} (Phase I: 40 to 70 dB_{AE}, 15 to 10^2 aJ), stabilised (Phase II: ca. 70 dB_{AE}, ca. 10^2 aJ) and increased suddenly before failure (Phase III: >70 dB_{AE}, 10^2 to 10^3 aJ. Although failure occurred in the mortar-brick interface, amplitude and energy levels during shear were generally lower than for the mortar cube (Figure 3). However, emission characteristics of shear and compression failure are likely to be different and require further investigation. It also needs to be noted, that intensity of the detected AE signals may be influenced by the orientation and polarization of AE sensor. R15α sensors used in the test series are polarized in the thickness direction and therefore more sensitive to longitudinal rather than shear waves.

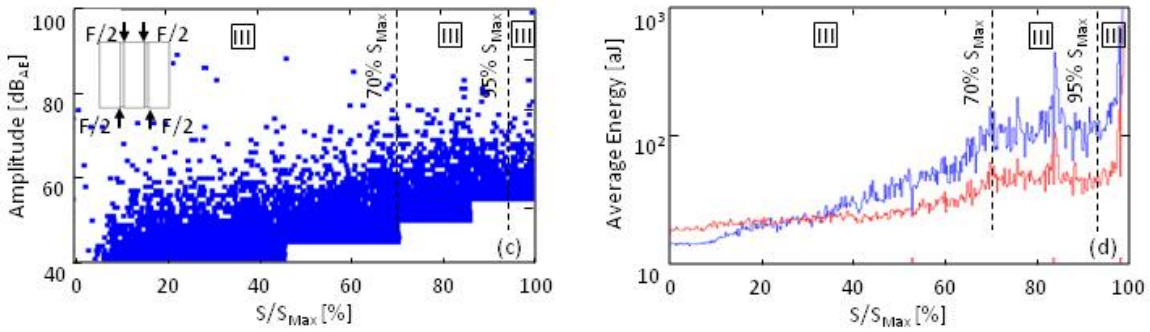

Figure 5: Triplet under shear: Amplitude vs. Stress (a); Average Energy (log) vs. Stress (b)

FATIGUE LOADING OF TRIPLETS AND SN CURVES

Fatigue loading was applied as sinusoidal cyclic loading at 2 Hz frequency for a minimum of 3 million cycles, unless failure occurred previously. The load was applied between a minimum and maximum stress level (S_{Min}, S_{Max}), defined as a percentage of the average ultimate static capacity (S_{Av}). S_{Min} is intended to represent the dead load of the bridge due to its self-weight and permanent loads, and S_{Max} the variation induced by passing traffic. For the test series S_{Min} was kept constant at 10% S_{Av}. The summary of the compression and shear test results is shown in Figure 6a and b for the maximum stress level (S_{Max}/S_{Av}) against the maximum number of cycles at failure (log) in the form of an S-N relationship. Static test results are indicated as failure at 1 cycle and specimens that did not fail are also included in the graph. While the number of cycles at failure generally increased for reduced stress levels, there is significant variability within the test results. The scatter is not surprising, as the fatigue stress level was defined as a percentage of the average static strength (S_{Av}) for a batch of samples and a selected fatigue stress level does not necessarily represent the actual stress level for the particular specimen. Due to the natural variability of masonry, it is therefore inherently impossible to define the relationship between the stress level and life expectancy as a simple deterministic relationship. Probabilistic analysis is therefore necessary to take the aleatoric uncertainties into account and enable a relationship to be established between stress levels and desired confidence levels [33].

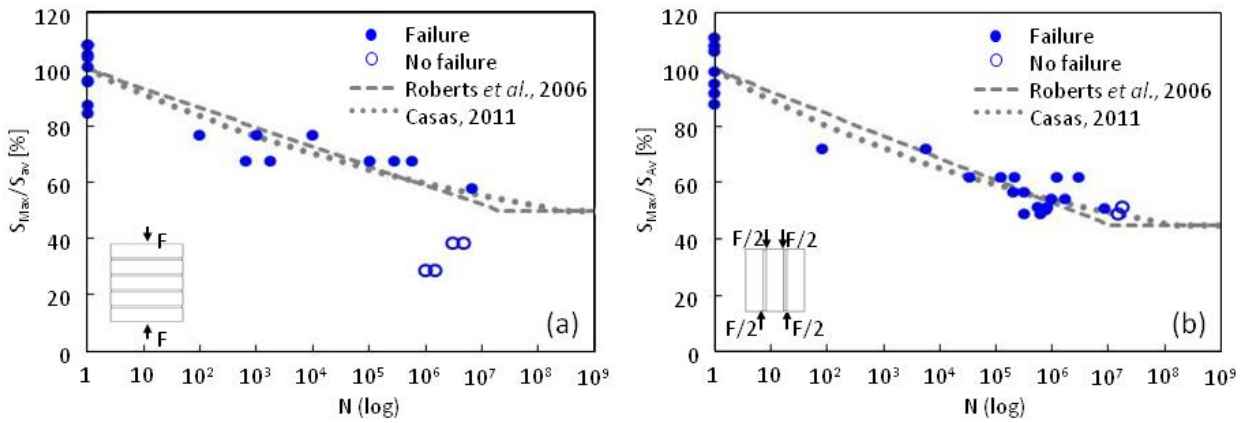

Figure 6: SN curves for a) compression and b) shear

Under compressive fatigue loading of a prism (for 10% - 80% S_{Av} loading range) a typical AE emission pattern is shown in Figure 7 for amplitude and energy against number of cycles (%). AE amplitude and energy both show a bathtub-type pattern, typically observed during creep deterioration [20,24] with with three distinctive regions:

- Phase I: reduction in high level emission up to ca. 28% of the total number of cycles (Phase I: 100-80 dB_{AE}, 10^7-10^5 aJ)
- Phase II: stabilised emission (Phase II: < 85 dB_{AE}, 10^5 aJ);
- Phase III: emission increase from ca. 67% of the total number of cycles leading to failure (Phase III: 80-90 dB_{AE}, 10^5-1.5x10^6 aJ).

Fatigue failure development is clearly visible during Phase III that can offer a highly useful warning period during monitoring to help avoid failure and collapse of the structure. It is also interesting to note, that in Phase II the emission stabilised to a level similar to 80% stress during static loading of a prism (Figure 4, ca. 85 dB_{AE}, 1.5x10^5 aJ).

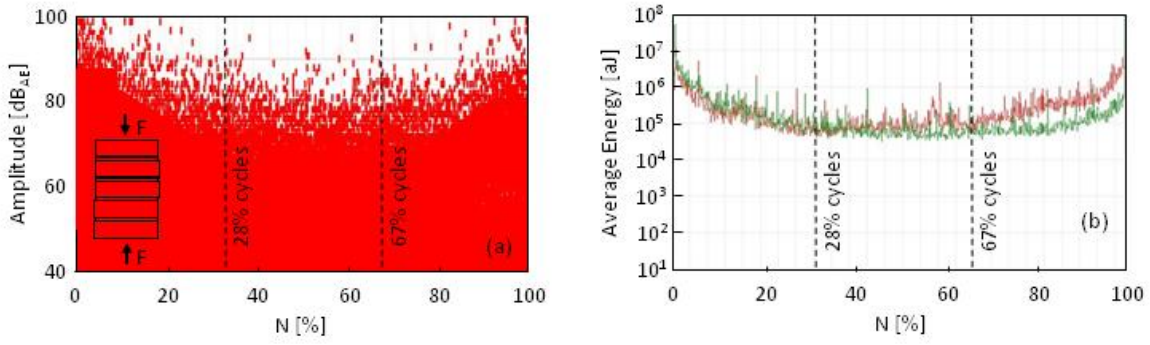

Figure 7: Prism under fatigue compression: Amplitude vs. Number of cycles (a); Average Energy (log) vs. Number of cycles (b)

A typical AE emission pattern during fatigue loading of a triplet under shear is shown in Figure 8 for 10% - 70% S_{Av} loading range. Similarly to fatigue compression, AE amplitude and energy also show a bathtub-type pattern, but only with two distinguishable phases: initial reduction, followed by increased emission from ca. 58% of the total number of cycles. As the emission settled around 58% of cycles, the amplitude is somewhat below the relevant level for 70% static loading of a prism (Figure 5) but the average energies is very similar (10^2 aJ).

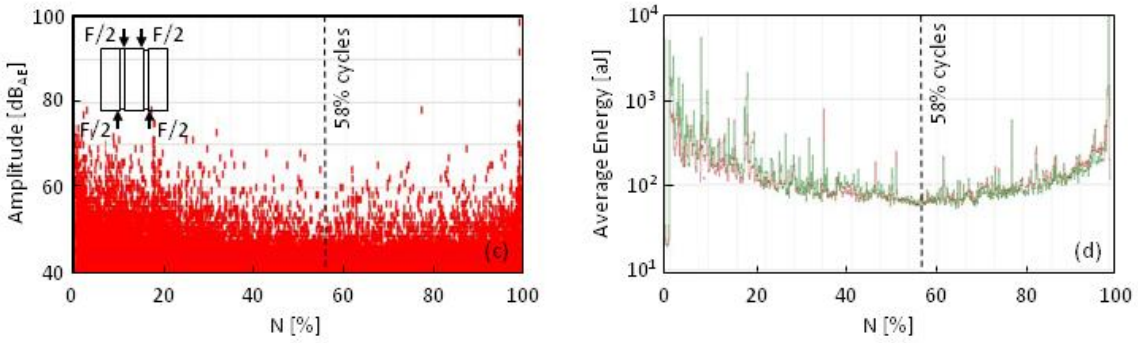

Figure 8: Triplet under fatigue shear: Amplitude vs. Number of cycles (a); Average Energy (log) vs. Number of cycles (b)

Indication of relevant emission levels between fatigue and static tests suggest the possibility to predict long-term fatigue emission levels and potentially life expectancy of specimens based on static test results. Similar relationship has been suggested by Antonaci [34] between static displacement and long-term fatigue behaviour of bricks, but further study is required to explore the issue in greater depth.

MATHEMATICAL MODELLING

In terms of mathematical relationship, S-N type models (Wöhler curves) have been proposed for the study of fatigue failure of brittle materials based on fracture mechanics principles (35), and a limited number of models have been specifically suggested for masonry. Roberts [1] proposed a lower bound fatigue limit with a linear relationship between the induced stress level and logarithm of the number of cycles, based on a series of small-scale laboratory tests [Equation 1]:

$$\frac{\left(\Delta S \cdot S_{Max}\right)^{0.5}}{S_{Av}} = k_1 - k_2 \cdot \log(N) > S_{FLS} \tag{1}$$

where ΔS is the stress range ($\Delta S = S_{Max} - S_{Min}$), S_{Max} the maximum stress, S_{Av} the quasi-static compressive strength, N the number of cycles, k_1 and k_2 are scalar parameters and S_{FLS} the stress level associated with the Fatigue Limit State. Static loading is represented as $N = 1$, for which $k_1 = (1 - S_{Min})^{0.5}$ and k_2 represent the slope of the linear S-N curve to provide best fit with the experimental data. For the current test results parameters $k_1 = 0.948$, $k_2 = 0.069$ and $S_{FLS} = 0.5$ have been identified for compression and $k_1 = 0.948$, $k_2 = 0.079$ and $S_{FLS} = 0.45$ for shear. The proposed fatigue relationship is also included in Figures 6a and b together with the experimental test data to demonstrate the methodology. Large amount of data is however needed to enable the fatigue behaviour of masonry to the quantified that is outside the scope of the present paper.

The fatigue model suggested by Casas [33] was based on the statistical analysis of the experimental results by Roberts [1] and was developed specifically for probabilistic analysis of masonry arch bridges [Equation 2]:

$$\frac{S_{Max}}{S_{Av}} = A \cdot N^{-B(1-R)} > S_{FLS} \quad (2)$$

where N is the number of cycles, R is the ratio of the minimum stress to the maximum stress ($R = S_{Min} / S_{Max}$), A and B are scalar parameters and S_{FLS} the stress level associated with the Fatigue Limit State. The exponent of N is a function of S_{Min} that enables the slope of the curve to be adjusted for various base loads. For static tests with $N = 1$ and $S_{Max} = S_{Av}$, the value for A is set to 1. For the current test data the value of B is identified as 0.045 for compression and 0.055 for shear and the model is also indicated in Figures 6a and b.

LIMIT STATES

The fatigue limit is generally considered a safe limit below which no failure occurs for a theoretically unlimited number of cycles. While it is quick and easy to produce fatigue test data for high stress levels, producing test results for relatively low stress levels is far more challenging due to excessive time requirements. Realistically, 10^8 cycles would be around the time limit that could be tested under laboratory conditions (ca. 9 month, 4 Hz) that would still be insufficient to identify the existence of a long-term fatigue limit for masonry. Similarly to plain concrete that does not appear to have a fatigue limit [36], the existence of a fatigue limit cannot be confirmed for masonry either, based on the available literature. In terms of practical application for masonry bridges, a permissible limit state (PLS) has been proposed as a safe limit at which there is a loss of structural integrity that will measurably affect the ability of the bridge to carry its working loads for the expected life of the bridge [12]. The permissible limit may be defined by the maximum possible number of cycles during the expected lifespan of a structure (e.g., number of vehicles/axles over a bridge). For example, for an expected 300 years life-expectancy of a masonry arch bridge, under non-realistic constant 24/7 loading at 2 Hz, the maximum number of cycles would not exceed ca. $2x10^{10}$. With the help of S-N curves and probability analysis, the predicted stress level for the maximum possible number of cycles could therefore be taken as a permissible limit for the specific application. Although there is insufficient fatigue test data available at the moment to quantify the permissible limit for masonry, the available information is intended to be used to demonstrate the methodology.

CONCLUSIONS

The deterioration process of medium-strength brick masonry was investigated through a series of small-scale laboratory tests under compression and shear with the help of acoustic emission (AE) monitoring, to investigate the likely deterioration mechanisms under static and fatigue loading.

- Stages of compaction, micro-cracking and macro-cracking were identified for bricks, mortar, prisms and triplets during static and fatigue loading with the help of AE monitoring.
- AE technique was shown to be capable of recording internal crack development and warn of imminent failure well before any sign of damage could be visually observed on the surface. AE monitoring has great potentials for field monitoring to warn of imminent failure or collapse.
- Fatigue test results were presented in the form of S-N curves for compression and shear and mathematical relationships were proposed based on existing models.
- No evidence of a Fatigue Limit State has been identified for masonry in the test series or in the literature. Instead, the methodology for a more relevant Permissible Limit State has

been demonstrated for masonry arch bridges that can help estimate critical stress levels and remaining life expectancy.

The paper attempts to present qualitative insight into the fracture development process of masonry and demonstrate a possible methodology, but further work is required to enable quantitative analysis.

ACKNOWLEDGEMENTS

The authors gratefully acknowledge the financial support of EPSRC.

REFERENCES

1 Roberts, T.M., Hughes, T.G., Dandamudi, V.R. and Bell, B. (2006) "Quasi-static and high cycle fatigue strength of brick masonry" Construction and Building Materials 20(9): 603-614.

2 Abrams, D.P., Noland, J.L. and Atkinson, R.H. (1985) "Response of clay-unit masonry to repeated compressive forces" 7th International Brick Masonry Conference, Melbourne, p. 567-576.

3 Brencich, A., de Felice G. (2009) "Brickwork under eccentric compression: Experimental results and macroscopic models" Construction and Building Materials 23(5): 1935-1946.

4 Ronca P., Franchi A., Crespi P. Structural failure of historic buildings: masonry fatigue tests for an interpretation model, in 4th International Conference on Structural Analysis of Historical Constructions, Modena C., Lourenço P.B., Roca P., Editors. Taylor and Francis: Padova, Italy. 2005. p. 273-279.

5. AlShebani, M., Sinha, S. (1999) "Stress-strain characteristics of brick masonry under uniaxial cyclic loading" ASCE Journal of Structural Engineering 125(6): 600-604.

6 Tomor, A.K., Wang, J. (2010) "Fracture development process for masonry under static and fatigue loading" 6th International Conference on Arch Bridges: Fuzhou, China, p. 550-560.

7 Wang, J., Tomor, A.K., Melbourne, C. and, Yousif, S. (2013) "Critical review of research on high-cycle fatigue behaviour of brick masonry" Construction and Building Materials, 38: 602–609

8 Melbourne, C., Tomor, A.K. and Wang, J. (2004) "Cyclic load capacity and endurance limit of multi-ring masonry arches" 4th Arch Bridges Conference: Barcelona, p. 375-384.

9 Clark, G.W. (1994) "Bridge analysis testing and cost causation project: serviceability of brick masonry" British Rail Research Report, LR CES 151.

10 Choo, B.S., Hogg, V. (1995) "Determination of the serviceability limit state for masonry arch bridges" Arch Bridges (Melbourne C (ed.)), Thomas Telford, London, UK. p. 529-536.

11 Melbourne, C., Tomor, A.K. and Wang. J. (2004) "Cyclic load capacity and endurance limit of multi-ring masonry arches" Proceedings of 4th Arch Bridges Conference (Roca P and Oñate E (eds)), CIMNE, Barcelona, Spain. p. 375-384.

12 Melbourne. C., Tomor, A.K. and Wang, J. (2007) "A New Masonry Arch Bridge Assessment Method (SMART)" Proceedings of the Institution of Civil Engineering – Bridge Engineering 160(2): 81-87.

13 BD 21/01 (2001) "The Assessment of Highway Bridges and Structures" Department of Transport, UK.

14 BA 16/97 (1997) "The Assessment of Highway Bridges and Structures" Department of Transport, UK.

15 Harvey, W.J. (1988) "Application of the mechanism analysis to masonry arches" The Structural Engineer, 66(5): 77-84.

16 Gilbert, M., Melbourne, C. (1994) "Rigid-block analysis of masonry structures" Structural Engineering, 72(21): 356-361.
17 Fanning, P.F., Boothby, T.E. (2001) "Three-dimensional modelling and full-scale testing of stone arch bridges" Computers and Structures, 79(29-30): 2645-2662.
18 Brencich, A. De Francesco, U. (2004) "Assessment of multispan masonry arch bridges. I: simplified approach" ASCE Journal of Bridge Engineering, 9(6): 582-590.
19 De Felice (2009) "Assessment of the load-carrying capacity of multi-span masonry arch bridges using fibre beam elements" Engineering Structures, 31(8): 1634-1647.
20 Verstrynge, E., Schueremans, L., Van Gemert. D. and Wevers, M. (2009) "Monitoring and predicting masonry's creep failure with the acoustic emission technique" NDT&E International 42(6): 518-523.
21 Verstrynge, E., Ignoul, S., Schueremans, L., Van Gemert, D. and Wevers, M. (2008) "Application of the acoustic emission technique for assessment of damage accumulation in masonry" Int J Restor Build Monum, 14(3): 167-78.
22 Melbourne, C., Tomor, A.K. (2006) "Application of acoustic emission for masonry arch bridges" Strain, 42(3): 165-72.
23 Tomor, A.K., Melbourne, C. (2007) "Condition monitoring of masonry arch bridges using acoustic emission techniques" Structural Engineering International, 17(2): 188-92.
24 Carpinteri, A., Lacidogna, G. and Pugno, N. (2007) "Structural damage diagnosis and life-time assessment by acoustic emission monitoring" Engineering Fracture Mechanics, 74(1-2): 273-289.
25 Carpinteri, A., Lacidogna, G. (2006) "Damage monitoring of an historical masonry building by the acoustic emission technique" Materials and Structures, 39(2): 161-7.
26 Shigeishi, M., Colombo, S., Broughton, K.J. et al. (2001) "Acoustic emission to assess and monitor the integrity of bridges" Construction and Building Materials, 15(1): 35-49.
27 De Santis, S. Tomor, A.K. (2013) "Laboratory and field studies on the use of acoustic emission for masonry bridges" NDT&E International, 55: 64-74.
28 Masera, D., Bocca, P. and Grazzini, A. (2011) "Frequency Analysis of Acoustic Emission Signal to Monitor Damage Evolution in Masonry Structures" 9th International Conference on Damage Assessment of Structures (DAMAS 2011), Journal of Physics: Conference Series 305.
29 Grosse, C.U., Ohtsu, M., eds. (2008) "Acoustic emission testing - basics for research - applications in civil engineering" Springer.
30 BSI (2009) "BS EN 1330-9:2009 Non-destructive testing. Terminology. Terms used in acoustic emission testing" BSI, London, UK.
31 BSI (2010) "BS EN 13477-2:2010, Non-destructive testing. Acoustic emission. Equipment characterisation. Verification of operating characteristic" BSI, London, UK
32 Schueremans, L. (2001) "Probabilistic evaluation of structural unreinforced masonry" PhD Thesis. Civil Engineering Department, KU Leuven.
33 Casas, J.R. (2011) "Reliability-based assessment of masonry arch bridges" Construction and Building Materials, 25(4): 1621-1631.
34 Antonaci, A., Bocca, P. and Masera, D. (2011) "Cyclic vs. static loading behaviour of masonry blocks: an approach to evaluate the long-term behaviour" Key Engineering Materials, 452-453: 129-132.
35 Carpinteri, A., Paggi, M. (2009) "A unified interpretation of the power laws in fatigue and the analytical correlations between cyclic properties of engineering materials" International Journal of Fatigue, 31(10): 1524-1531.

36 Lee, M.K., Barr, B.I.G. (2004) “An overview of the fatigue behaviour of plain and fibre reinforced concrete” Cement & Concrete Composites, 26(4): 299-305.